MFN 07-612

Enclosure 2

NEDO-33244, Revision 1,
"ESBWR Marathon Control Rod Mechanical Design Report,"
November 2007

Non-Proprietary Version

HITACHI

*GE Hitachi Nuclear Energy*

**NEDO-33244 Revision 1**
**DRF 0000-0075-2316**
**Class I**
**November 2007**

# LICENSING TOPICAL REPORT

# ESBWR MARATHON CONTROL ROD MECHANICAL DESIGN REPORT

# NON-PROPRIETARY INFORMATION NOTICE

This is a non-proprietary version of the document NEDE-33244P, Revision 1 which has the proprietary information removed. Portions of the document that have been removed are indicated by open and closed double brackets as shown here [[ ]].

## IMPORTANT NOTICE REGARDING CONTENTS OF THIS REPORT

**Please read carefully**

The information contained in this document is furnished **for the purpose of supporting the NRC review of the certification of the ESBWR**, with the information here being used as ABWR supporting reference. The only undertakings of GE-Hitachi Nuclear Energy (GEH) with respect to information in this document are contained in contracts between GEH and any participating utilities, and nothing contained in this document shall be construed as changing those contracts. The use of this information by anyone other than that for which it is intended is not authorized; and with respect to **any unauthorized use**, GEH makes no representation or warranty, and assumes no liability as to the completeness, accuracy, or usefulness of the information contained in this document.

## Table Of Contents

## List of Tables

## List of Figures

## ACRONYMS AND ABBREVIATIONS

| Acronym / Abbreviation | Description |
|---|---|
| AOO | Anticipated operational occurrence |
| ASME | American Society of Mechanical Engineers |
| ATWS | Anticipated Transient Without Scram |
| CFR | Code of Federal Regulations |
| CRB | Control rod blade |
| DCD | Design Control Document |
| FMCRD | Fine Motion Control rod drive |
| CRDA | Control Rod Drop Accident |
| ECCS | Emergency core cooling system(s) |
| ECP | Engineering Computer Code |
| ESF | Engineered Safety Feature |
| FHA | Fuel Handling Accident |
| GEH | General Electric -Hitachi Nuclear Energy |
| GNF | Global Nuclear Fuels |
| IASCC | Irradiation Assisted Stress Corrosion Cracking |
| LOCA | Loss of Coolant Accident |
| LTR | Licensing topical report |
| MCPR | Minimum Critical Power Ratio |
| MSLBA | Main Steamline Break Accident |
| NRC | U.S. Nuclear Regulatory Commission |
| OBE | Operating Basis Earthquake |
| QA | Quality assurance |
| RAI | Request for additional information |
| SRSS | Square root sum of squares |
| SSE | Safe Shutdown Earthquake |
| STS | Standard Technical Specifications |
| TS | Technical Specifications |

## EXECUTIVE SUMMARY

The GEH ESBWR Marathon control rod is a derivative of the BWR/2-6 Marathon design approved by Reference 1. The primary difference between the ESBWR Marathon and the BWR/2-6 Marathon design is a shorter absorber section appropriate for ESBWR application. The ESBWR Marathon design uses the same square absorber tube design, as the BWR/2-6 Marathon design, approved in Reference 1.

The ESBWR Marathon control rod uses a boron carbide ($B_4C$) capsule with the same cross-sectional dimensions as the Marathon-5S control rod (Reference 3). Compared to the original BWR/2-6 design (Reference 1), the ESBWR capsule has [[

]]

The structure of the ESBWR Marathon control rod has been evaluated during all normal and upset conditions, and has been found to be mechanically acceptable. The fatigue usage of the control rod has also been found to be well below lifetime limits.

[[

]] For all cases, the mechanical lifetime exceeds the nuclear lifetime. Therefore, the ESBWR Marathon control rod is nuclear lifetime limited.

The licensing acceptance criteria contained in the ESBWR Design Control Document (Reference 4) are evaluated and are judged to be sufficient and complete. The nuclear analysis of the ESBWR Marathon control rod is described in Reference 5. GEH requests NRC approval for the use of the Marathon control rod for ESBWR.

# 1. INTRODUCTION AND BACKGROUND

This report contains ESBWR Marathon control rod mechanical analysis results. This report represents a complete revision of the NEDE-33244P revision 0 report, incorporating changes to the control rod design.

GEH currently manufactures the long life Marathon Control Rod Blade (CRB) for BWR/2 through BWR/6. The Nuclear Regulatory Commission (NRC) acceptance of the Marathon CRB is documented by a Licensing Topical Report (LTR), Reference 1. The Marathon CRB consists of 'square' absorber tubes, edge welded together to form the control rod wings, and welded to individual tie rod segments to form the cruciform assembly shape. The square absorber tubes are filled with a combination of boron carbide ($B_4C$) capsules, empty capsules, hafnium rods, and spacers. Previously, GEH manufactured original equipment and replacement Duralife Control Rod Blades, which consisted of a full-length tie rod, with boron carbide absorber rods and hafnium plates and/or strips enclosed within a sheath to form each wing. The most recent Duralife Licensing Topical Report is shown as Reference 2.

The design presented in this report is the Marathon control rod, adapted for use in ESBWR. The following sections contain the mechanical analysis of the Marathon control rod for application to ESBWR. The nuclear analysis is contained in Reference 5.

GEH requests NRC approval for the use of the ESBWR Marathon control rods.

# 2. DESIGN CHANGE DESCRIPTION

The basic design of the ESBWR Marathon is the same as the BWR/2-6 Marathon approved by Reference 1. The control rod wings consist of edge welded square absorber tubes (Figure 2-1). The ESBWR Marathon control rod is an all boron carbide design as all tubes are filled with either boron carbide capsules, or empty capsule plenums. As in the BWR/2-6 Marathon design, the ESBWR capsules use a crimped capsule end cap connection.

There are six design changes made to the BWR/2-6 Marathon CRB, as described in Reference 1, to produce the ESBWR Marathon CRB. These changes are described in the following subsections.

## 2.1 ABSORBER SECTION LENGTH

Since the active fuel height of the ESBWR design is shorter than BWR/2-6, the active absorber zone for the control rod is also shorter. As shown in Table 2-1 of Reference 1, the nominal length of the BWR/2-6 Marathon absorber section is [[ ]]. For the ESBWR version, this is reduced to [[ ]]. This value is reflected in Table 2-1.

## 2.2 CAPSULE GEOMETRY

The ESBWR Marathon CRB uses a capsule body tube geometry with [[ ]]. The cross-sectional dimensions of the ESBWR capsule are identical to the capsule for the Marathon-5S design described in Reference 3.

A comparison of the ESBWR and the BWR/2-6 Marathon capsule dimensions is contained in Table 2-1. Due to irradiation induced $B_4C$ powder swelling, a $B_4C$ capsule expands as the absorber is depleted. [[ ]]. This is discussed in more detail in Section 3.6

## 2.3 CAPSULE LENGTH

The BWR/2-6 Marathon CRB LTR (Reference 1) identifies the nominal length of the $B_4C$ capsules as 11.4 inches. Current BWR/2-6 Marathon CRB designs use 36” capsules [[ ]] and 24” [[ ]] $B_4C$ capsules. [[

]]

Due to the reduced length of the ESWR absorber section, the length of the capsules is also reduced. The ESBWR design uses nominal length [[ ]] boron carbide capsules. These capsule lengths are reflected in Table 2-1. A diagram of the absorber section load pattern is shown in Figure 2-2.

## 2.4 CONNECTOR

To be compatible with the ESBWR Fine Motion Control Rod Drive (FMCRD), the ESBWR Marathon control rod uses a connector, rather than a velocity limiter, as shown in Figures 2-3 and 2-4.

## 2.5 HANDLE WITH SPACER PADS

The Marathon LTR (Reference 1) allows for the use of the traditional handle with rollers or handles with wear pads. To eliminate the possibility of stress corrosion cracking initiating within the handle pin-hole, the ESBWR Marathon control rod employs a raised spacer pad, similar to what is currently being used for D lattice (BWR/2-4) Marathon control rod applications. The raised spacer pad is shown in Figure 2-4.

## 2.6 FULL LENGTH TIE ROD

The BWR/2-6 Marathon CRB uses multiple tie rod segments along the center of the cruciform shape. The ESBWR Marathon CRB utilizes a single tie rod that runs the entire length of the assembly similar to that used on Duralife control rods (see Reference 2). The cross-sectional geometry of this full-length tie rod is designed such that it does not alter the interface between the control rod and the adjacent fuel channels. This is achieved by ensuring that contact occurs between the wing of the control rod and the face of the fuel channel and not at the fuel channel corner and tie rod.

A cross-section of the ESBWR Marathon control rod is shown in Figure 2-1.

**Table 2-1**
**Comparison of Typical Parameters of Marathon and ESBWR Marathon CRBs**

| Parameter | BWR/6 Marathon CRB [1] | ESBWR Marathon CRB |
|---|---|---|
| **Control Rod Weight** (lb) | [[ | |
| **Absorber Tubes per Wing** | | |
| **Nominal Wing Thickness** (in) | | |
| **Absorber Tube** | | |
| Length (in) | | |
| Inside Diameter (in) | | |
| Nominal Thin Section Wall Thickness (in) | | ]] |
| Material | 304S | 304S |
| Cross-sectional area (in$^2$) | [[ | ]] |
| **$B_4C$ Absorber Capsule** | | |
| Length (in) | [[ | |
| Inside Diameter (in) | | |
| Wall Thickness (in) | | |
| Material | | |
| B4C Density (g/cc) | | |
| B4C Density (% theoretical) | | ]] |

1. Values from Table 2-1 of the Marathon LTR (Reference 1), except for absorber tube cross-sectional area from design calculations. Current Marathon absorber capsule lengths are also updated, see Section 2.3.
2. [[ ]].

[[

]]

**Figure 2-1. ESBWR Marathon CRB Cross-Section**

[[

]]

Figure 2-2. ESBWR Marathon Control Rod Load Pattern

# 3. SYSTEM DESIGN

## 3.1 ANALYSIS METHOD

For each control rod load application, worst case or bounding loads are identified. Stresses are calculated using worst-case dimensions and limiting material properties. For analyses involving many tolerances, square root sum of squares (SRSS) or statistical tolerancing may be used.

### 3.1.1 Combined Loading

As in Reference 1, effective stresses and strains are determined using the distortion energy theory (Von Mises), and compared to allowable limits. Using the principal stresses: $\sigma_1$, $\sigma_2$, and $\sigma_3$, the equivalent Von Mises stress is calculated as:

$$\sigma_{VM} = \sqrt{1/2[(\sigma_1 - \sigma_2)^2 + (\sigma_2 - \sigma_3)^2 + (\sigma_3 - \sigma_1)^2]}$$

Both the Von Mises and Tresca stress criteria are used to predict the conditions for yielding under both uniaxial and multiaxial stress states. The Tresca Criterion can be called the maximum shear criterion since it measures the maximum shear stress present The Von Mises takes into account all principal stresses in the calculation of the conditions where yielding occurs. For thin walled tubes, under combined loads, the Von Mises Criterion appears to more accurately represent the condition under which yielding occurs (Reference 11). The use of the Von Mises criterion takes into consideration the hydrostatic component of stress and the corresponding strain value. It should be recognized that failure modes in thin walled structures such as control rod absorber tubes are initiated at the surface, a location where one of the three principal stresses is zero. The use of the von Mises criterion is therefore adequate to evaluate the potential for any of the important failure modes. First, ductile failure is associated with plastic flow. The criterion was developed to best assess that mode. Fatigue and crack growth processes would initiate on the surface. Again, plastic flow at the surface is necessary for these processes to start. As supported by the stress analyses results in Section 3.3 through 3.8, the stresses are below the un-irradiated stress limits. Therefore, the absorber tubes will only experience elastic deformation. This condition is also true in the irradiated condition where the stress ratio will decrease when compared to the actual irradiated yield strength value.

Given this, the effects of irradiation are well known. Specifically, the material will have a significant increase in yield strength and ultimate strength. Therefore, the design criteria used, one based on un-irradiated properties, will insure that as fluence is accumulated, the component continues to remain elastic and well below the actual yield strength. As stated in Reference 1, this approach has been previously accepted.

### 3.1.2 Unirradiated Versus Irradiated Material Properties

Each structural analysis is first evaluated to determine whether unirradiated or irradiated material properties are appropriate. In general, as stainless steel is irradiated, the yield and ultimate tensile strengths increase, while the ductility, or allowable strain decreases. In order to determine the correct technique, the analyses are divided into two categories:

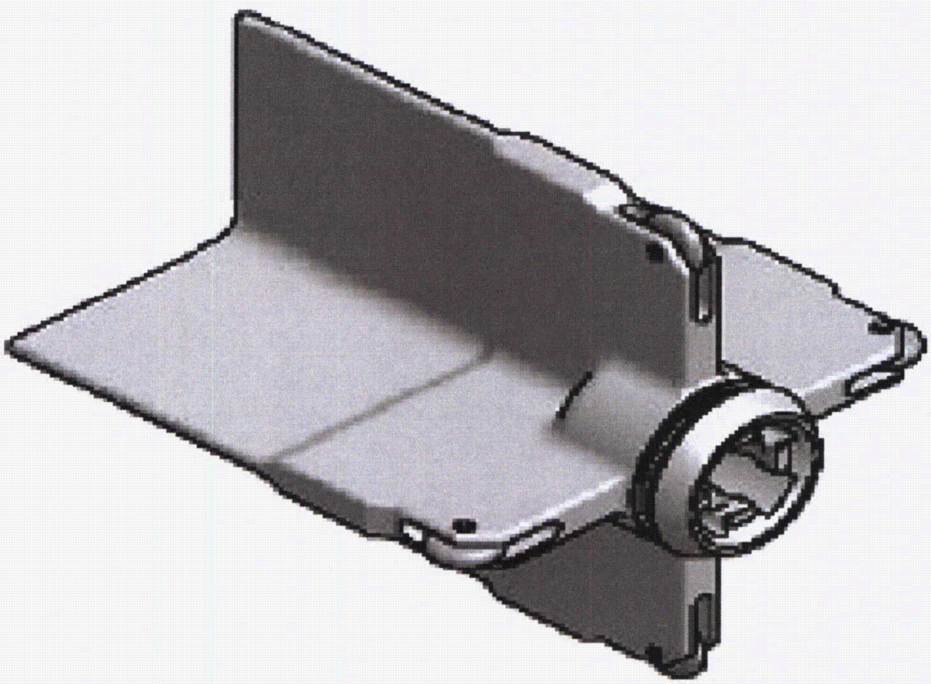

**Figure 2-3. ESBWR Marathon Connector**

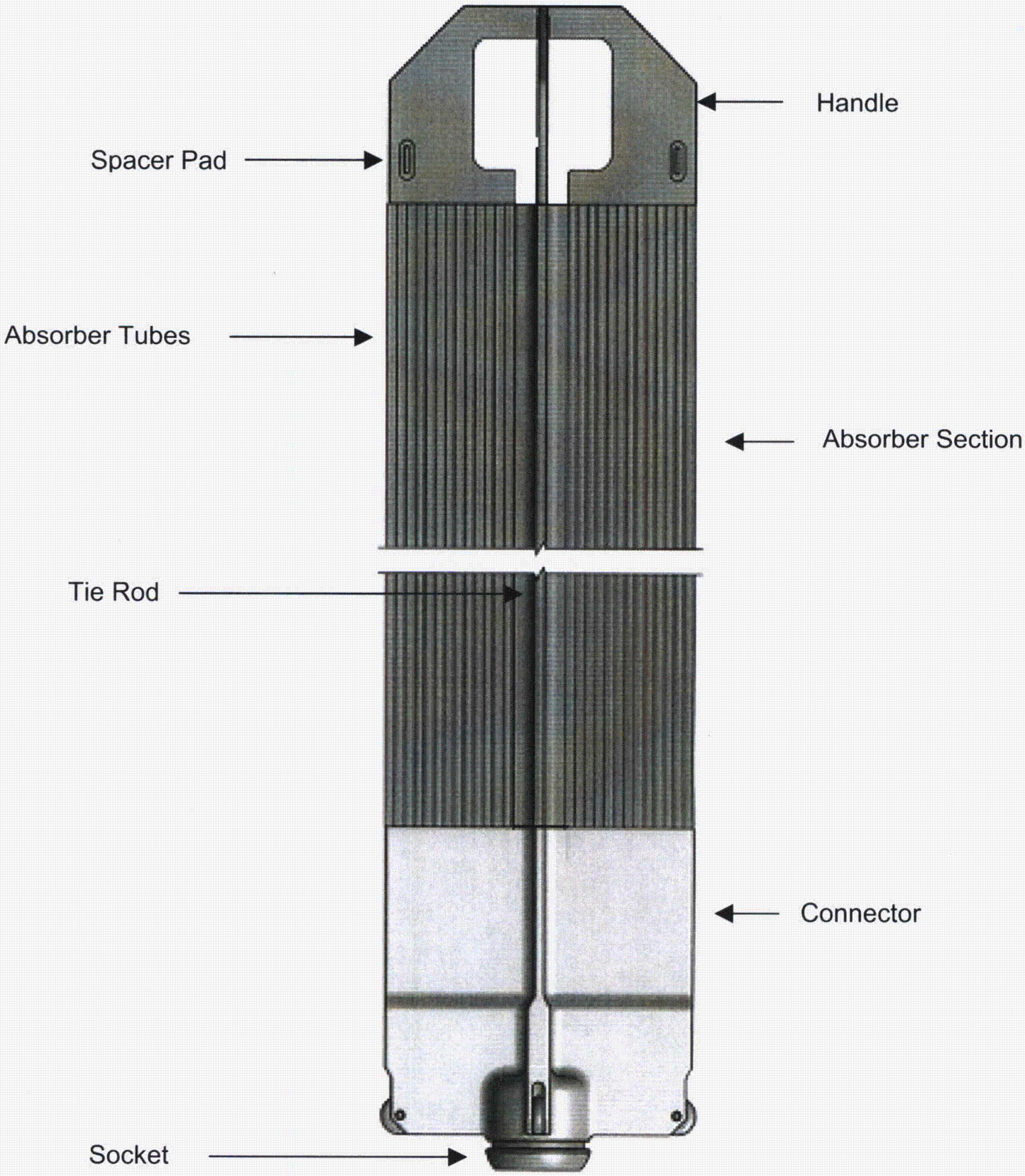


**Figure 2-4. ESBWR Marathon Control Rod**

1. Analyses with an applied load (i.e., scram). For these analyses, a maximum stress is calculated, and compared to the limiting unirradiated stress limit.
2. Analyses with an applied displacement (i.e., seismic bending). For these analyses, a maximum strain is calculated, and compared to the limiting irradiated strain limit.

Austenitic stainless steels do not display a ductile to brittle transition (DBTT). The material fracture toughness and ductility (in the unirradiated condition) does not vary significantly in the temperature range of interest (70 - 550°F). In turn, the effect of irradiation on austenitic stainless steel is to reduce the toughness and ductility somewhat; however, austenitic stainless steel still retains ductility after irradiation. There are existing data at high fluence that confirm the tensile ductility and fracture toughness. Specifically, ductility levels and fracture toughness data for irradiated components are documented in Reference 9. These data substantiate their ductile behavior at both room temperature as well as operating temperature.

## 3.2 MATERIAL PROPERTY LIMITS

The limiting unirradiated material strengths are first identified for the control rod structural materials, and shown in Table 3-1. For most materials, limiting values from the ASME Boiler and Pressure Vessel Code are used. In other cases, minimum material strengths are specified in GEH material specifications.

GEH requires that the mechanical properties of all material used in the fabrication of control rods be certified as meeting material specification limits. For example, the mechanical properties of finished, annealed, and un-irradiated type 304S absorber tubes are defined by a fabrication specification. These mechanical limits, along with the certification results of three recent absorber tube lots are shown in Table 3-22. As shown, all mechanical properties meet the specification requirements. See section 3.2.4 for more information on GEH's stabilized type 304S stainless steel.

### 3.2.1 Stress Criteria

The licensing acceptance criteria of Appendix 4C of Reference 4 are used, in which the control rod stresses and strains and cumulative fatigue shall be evaluated to not exceed the ultimate stress or strain of the material, structure, or welded connection.

The figure of merit employed for the stress-strain limit is the design ratio, where:

Design ratio = effective stress/stress limit, or, effective strain/strain limit.

The design ratio must be less than or equal to 1.0. Conservatism is included in the evaluation by limiting stresses for all primary loads to one-half of the ultimate tensile value.

Resulting allowable stresses for primary loads are shown in Table 3-2.

### 3.2.2 Absorber Tube Material Isotropy

The irradiation resistant special melt austenitic stainless steel (type 304S) used for the control rod absorber tubes is manufactured using standard industrial processes and solution annealing.

There is no significant anisotropy produced in wrought product by these procedures. Photos of finished absorber tubes, at 300X magnification, in different orientations, are shown in Figures 3-14 through 3-16. The axial loading direction is the direction of design concern and is aligned with the direction of standard tensile tests on irradiated material. The necking observed in these irradiated tensile tests can be interpreted as supporting the adequacy of the strength and ductility of the material in the radial direction.

### 3.2.3 Welded Connections

For welded connections, a weld quality factor, q, is used to further reduce the allowable stress. Therefore, the allowable stress for a welded connection, Sm', is:

$$S_m' = (q)Sm$$

Weld quality factors are determined based on the inspection type and frequency of the weld. Weld quality factors are shown in Table 3-3.

### 3.2.4 Laser Welding Process

Laser Beam Weld (LBW) processes are used extensively in the manufacture of Marathon control rods. Welding processes for control rods are developed and qualified against a set of acceptance standards which includes: (1) meeting minimum penetration requirements, (2) smooth blends between welded members, and (3) no cracks, holes, lack of fusion or porosity. Since the ESBWR Marathon CRB uses the same square absorber tube as the BWR/2-6 Marathon CRB, the weld processes are the same.

As a result of the complexity of the control rod geometry, GEH qualifies the welding process in a manner meeting the intent of the ASME Code. The qualification method selected is to confirm the mechanical properties of the weld by using a representative mockup of the laser weld. Mechanical tests confirm that the mechanical properties of the weld were higher than the minimum properties of the base metal.

The weld quality factor (q) provides a safety margin against manufacturing defects during processing. The critical to quality components of the weld are defined by ASME B&PV code weld procedure QW-264.1, Welding Procedure Specifications, Laser Beam Welding (LBW). GEH further refines its internal critical to quality requirements from the ASME B&PV code for its day-to-day operations. [[
]]

GEH performs metallographic evaluation on sample laser welds on a weekly basis to confirm that the results of the welding process remain within parameters. These results are documented. Photomicrographs of a typical laser weld, taken as part of a recent qualification test, are shown in Figure 3-16. Comparing the grain structure at the edge of the weld to an area away from the weld shows that there is no effective heat affected zone for a laser weld. This combined lack of heat affected zone, Ta stabilization, and low carbon chemistry, accounts for the good carbide test results mentioned above.

Austenitic stainless steels have no inherent age hardening capability and lend themselves readily to the welding process. GEH's proprietary Type 304 S composition is as follows:

[[

]]

A common concern in austenitic stainless steel welds is carbide precipitation. Carbide formation in a weld heat affected zone would encourage intergranular stress corrosion cracking in this location. The combination of low heat input welding practices, tantalum stabilization, and restrictive carbon limits, provides an effective barrier to such intergranular cracking.

### 3.2.5 Absorber Tube Axial Shrink Due to Welding

Due to the absorber tube-to-tube laser welding process, the absorber tubes shrink by varying amounts in the axial direction. The resulting residual strain is evaluated using data from production BWR/2-6 Marathon control rods. Prior to welding, the length of the BWR/2-6 absorber tube is [[ ]]. The lengths of the absorber tubes after welding were measured on a production Marathon control, and are recorded in Table 3-23.

As shown in the table, the biggest difference in relative length between the absorber tubes after welding is [[ ]]

The length of the finished BWR/2-6 absorber section is [[ ]]. Therefore, the maximum axial strain due to the differential weld shrinking of the absorber tubes is:

Strain ($\varepsilon$)= $\Delta L/L_{initial}$ = [[ ]]

A [[ ]] strain is metallurgically insignificant in terms of driving microstructural changes in the bulk tubing. This strain is an elastic driver towards overall distortion. Distortion is minimized through production controls. Please see section 3.2.4 for further discussion with regard to the mechanical properties of the laser welds.

## 3.3 SCRAM

The largest axial structural loads on a control rod blade are experienced during a control rod scram, due to the high terminal velocity. To be conservative, structural analyses of the control rod are performed assuming a 100% failed control rod drive buffer. A dynamic model of mass, spring and gap elements is used to simulate a detailed representation of the load bearing components of the assembly during a scram event. Simulations are run at atmospheric temperatures, pressures, speeds, and properties as well at operating temperatures, pressures, speeds, and properties. The resulting loads are shown in Table 3-4.

Structural stresses are determined from the scram loads shown in Table 3-4 using the limiting material properties, weld quality factors, and worst-case geometry for the area subject to the load. Figure 3-1 shows the welds and cross-sections analyzed.

Resulting maximum stresses during a failed buffer scram are shown in Table 3-5. These stresses are evaluated against the stress limits shown in Table 3-2. Specific details for each calculation are shown in Appendix A. As shown by the design ratios in Table 3-5, sufficient margin exists against failure for all cross-sections and welds.

## 3.4 SEISMIC AND FUEL CHANNEL BOW INDUCED BENDING

Fuel channel deflections, which result from seismic events, impose lateral loads on the control rods. The ESBWR Marathon control rod is analyzed for the most limiting Safe Shutdown Earthquake (SSE) event.

### 3.4.1 Wing Outer Edge Bending

The SSE analysis is performed by evaluating the strain in the ESBWR Marathon absorber section with maximum SSE deflection. In addition, maximum control rod deflections due to fuel channel bulge and bow are conservatively added to the calculated seismic bending deflections. [[

]].

The limiting location for strain due to bending of the control rod cross-section occurs at the outer edge of the control rod wing. At this location, a combined strain due to simultaneous application of the following loads is calculated: (1) control rod bending due to an SSE seismic event, (2) control rod bending due to worst case channel bulge and bow, (3) axial absorber tube stress due to maximum internal pressure, and (4) a failed buffer scram. The results of these strain calculations are shown in Table 3-6. As shown, even under these combined worst-case conditions, the maximum strain is well below the limiting maximum allowable strain at irradiated conditions.

### 3.4.2 Absorber Tube to Tie Rod Weld

The combined effect of control rod bending due to SSE and channel bulge and bow deflection combined with maximum absorber tube internal pressure is also evaluated at the full-length tie rod to absorber tube weld. A finite element model is used, as shown in Figure 3-2. Resulting worst-case stresses are shown in Table 3-7. As shown, the resulting stresses are acceptable against the design criteria.

### 3.4.3 Absorber Tube Lateral Load

Finally, the lateral load imposed on the control rod absorber tube due to an excessively bowed channel is evaluated. The finite element model is shown in Figure 3-11. As shown, the entire lateral load is applied to the wear surface of a single square absorber tube, along with reactor internal pressure. For conservatism, no internal pressure is applied to the tube, which would offset the external pressure and reduce the stresses in the tube.

The resulting stress intensity plot is shown in Figure 3-12. The maximum stress intensity is calculated as [[ ]], which is less than the absorber tube allowable load of [[ ]] from Table 3-2.

The lateral load model is also evaluated using end-of-life irradiated material properties. This analysis is extremely conservative, since for the tube to be irradiated, there would be a corresponding build-up of internal pressure in the tube to offset the lateral load. However, for this model, no internal pressure is applied. The results of the calculation is a maximum stress intensity [[ ]], which is less than ½ of the irradiated true ultimate strength of the material of [[ ]]. Further, the maximum strain intensity is [[ ]], compared to an ultimate strain of [[ ]].

## 3.5 STUCK ROD COMPRESSION

Maximum compression loads from the Fine Motion Control Rod Drive (FMCRD) are evaluated for a stuck control rod. Both buckling, and compressive yield are analyzed for the entire control rod cross-section (buckling mode A), and conservatively assuming that the entire compression load is applied to a single control rod wing (buckling mode B). Figure 3-3 shows the buckling modes.

Results of the stuck rod compression loads are contained in Table 3-8 for the entire control rod cross-section (mode A), and in Table 3-9 for the single wing (mode B). As can be seen, neither compressive yielding nor buckling will occur for either buckling mode. Additionally, for both buckling modes, the compressive yield load is reached prior to the critical buckling load.

## 3.6 ABSORBER BURN-UP RELATED LOADS

The structure of a control rod must provide for positioning and containment of the neutron absorber material (Boron Carbide powder, Hafnium, etc) throughout its nuclear and mechanical life and prohibit migration of the absorber out of its containment during normal, abnormal, emergency and faulted conditions. The ESBWR Marathon CRB contains boron carbide powder within capsules contained within absorber tubes (capsule within a tube design).

The boron neutron absorption reaction releases helium atoms. Some of this helium gas is retained within the compacted boron carbide powder matrix, causing the powder column to swell. This swelling causes the $B_4C$ capsule to expand. The remainder of the helium is released as a gas. The capsule end caps for the ESBWR Marathon design are crimped to the capsule body tubes. This allows the helium gas to escape from the capsule and fill the absorber tube gap and any empty capsule plenum volume provided.

For the BWR/2-6 Marathon capsule design, [[

]].

For the ESBWR capsule design, [[

]].

Using the pressurization capability of the absorber tube, limits are determined for each absorber tube configuration (see Figure 2-2), in terms of $B_4C$ column depletion.

These individual absorber tube depletion limits are then combined with radial depletion profiles and axial depletion profiles to determine the mechanical depletion limit for the control rod assembly. See Section 3.9.

### 3.6.1 Irradiated Boron Carbide Swelling Design Basis

Mechanical test data of the irradiated behavior of boron carbide was obtained by irradiating test capsules for a period of approximately ten years in a reactor. Test capsules were placed in neutron monitor tubes and irradiated in a reactor. The configurations of two types of test capsules used are shown in Figure 3-7.

The dimensions of the test capsules were measured prior to irradiation, and post-irradiation in a hot cell using standard laboratory practice. For test capsules with a mandrel, the diametral strains were mathematically corrected to compensate for the mandrel, resulting in an increase of reported strain value.

Diametral swelling results are shown in the Table 3-15 and Figure 3-8. The ESBWR Marathon swelling analysis conservatively uses the $+3\sigma$ upper bound value of [[ ]].

Axial swelling data is shown in Table 3-16. As shown, the axial swelling is [[

]].

### 3.6.2 Clearance Between Capsule and Absorber Tube

As a result of the welding process forming the control rod wings, the inside diameter of the absorber tubes shrink. Therefore, a minimum inside diameter is established, and is 100% inspected following the welding, before the absorber section is loaded with capsules.

To evaluate the clearance between the capsule and absorber tube, worst-case capsule dimensions are used, which result in the maximum outside diameter at 100% local depletion. These consist of the original maximum outside diameter, and minimum wall thickness, resulting in the maximum beginning boron carbide diameter

The strain at the ID of the capsule is equal to the diametral strain of the boron carbide powder. The +3σ upper limit of [[ ]] from Table 3-15 is used. Then, assuming constant volume deformation of the capsule, the strain on the outside diameter of the capsule is:

[[ ]].

Then, the capsule outside diameter at 100% local depletion is:

$OD_{100\%} = OD_0(1+ \varepsilon_{OD})$.

A summary of this calculation is shown in Table 3-17. As shown, at 100% local depletion, using worst-case capsule and absorber tube dimensions and a conservative boron carbide swelling basis, a clearance exists between the capsule and the absorber tube. Therefore, there is no strain placed on the outer absorber tube due to boron carbide swelling.

### 3.6.3 Thermal Analysis

Pressure in the absorber tube due to helium release is calculated accounting for worst-case capsule and absorber tube dimensions and $B_4C$ helium release fraction. Because the fraction of helium released from the $B_4C$ powder increases with temperature, a finite element thermal analysis is performed to determine the peak $B_4C$ temperature (see Figure 3-5). This thermal analysis is performed using worst-case dimensions, maximum end-of-life crud buildup, combined with maximum beginning-of-life heat generation.

For the thermal model, corrosion is modeled as the build-up of an insulating layer of crud. This crud may be corrosion products from the control rod absorber tube, or deposited from other reactor internals. For all thermal analyses, a [[ ]] thick crud layer is applied, which is twice that assumed for the BWR/2-6 Marathon design.

A temperature distribution is shown in Figure 3-5. The model used assumes that the tube is interior to the wing, in that there is another absorber tube to the left and right. The boundary on the left and right is conservatively assumed to be insulated (zero heat flux).

Results of the thermal analysis are shown in Table 3-10, and in Figure 3-5. The following conservatisms are applied to the thermal model:

- Peak beginning-of-life heat generation rates are used, these are combined with:
- End-of-life combined corrosion and crud build-up of [[ ]], twice that used in previous analyses.
- Peak heat generation rates are used from the highest heat generation tube, which is actually the outermost edge tube. In reality, this tube will have coolant on one side, rather than be insulated. Further some heat transfer will occur from the peak heat generation tube to the adjacent tube, rather than be perfectly insulated.
- Maximum wall thickness dimensions are used.

Peak $B_4C$ temperatures are shown in Table 3-10. The temperatures shown in this table are based on peak beginning-of-life boron carbide heat generation rates (see Reference 5), and are from the peak heat generation absorber tube at the peak axial location. They are radially averaged only across the cross-section of an individual boron carbide capsule.

Helium release fractions are based on models developed using data from multiple sources. The data shows a significant dependence of helium release fraction on the irradiation temperature. The helium release fractions used are shown in Table 3-10. The helium release model is based on data from 500 °F to 1000 °F, which envelopes the temperatures shown in Table 3-10.

### 3.6.4 Absorber Tube Pressurization Capability

[[

]] Finite element analyses are performed to determine the pressurization capability of the absorber tube.

The burst pressure is defined as the internal pressure at which any point in the tube reaches a stress intensity equal to the true ultimate strength of the material. Then, to calculate an allowable pressure, a safety factor of 2.0 is applied to the differential pressure across the absorber tube wall such that:

$$P_{allow} = \frac{(P_{burst} - P_{external})}{2} + P_{external}$$

The burst pressure capability of the tube is initially calculated using square absorber tube nominal dimensions. The resulting burst pressure is then scaled down by [[ ]] to match burst pressure testing results. The nominal dimension and scaled burst pressures are shown in Table 3-20.

The pressurization analysis is then performed at worst-case drawing dimensions. The resulting burst pressure is shown in Table 3-20. As shown, although the burst pressure is less than the nominal case, it is bounded by the scaled burst pressure used to determine the tube allowable pressure. Therefore, the design basis absorber tube allowable pressure is conservative.

The effect of the welded connection of the innermost absorber tube to the tie rod is evaluated by modifying the pressurization model to incorporate the tie rod (Figure 3-10). The resulting burst pressure for this model is shown in Table 3-20. As shown, the burst pressure is less than the nominal, single tube value. However, it is bounded by the scaled burst pressure used to determine the absorber tube allowable pressure. Therefore, the design basis absorber tube allowable pressure is conservative.

Maximum Stress Components

Stress components at the point of maximum stress intensity were analyzed for the absorber tube with the maximum allowable internal pressure. The point of maximum stress intensity is found to be on the inside surface of the absorber tube. Principle stress components are shown in Table

3-18. All stress values shown in Table 3-18 are within the allowable stress value for 304S tubing of [[ ]] shown in Table 3-2.

Effect of the Welded Connection Between Absorber Tubes

The Marathon Control Rod Blade (CRB) is manufactured using very low heat input laser weld processes. The resulting regions of microstructural change including the associated heat affected zones (HAZ) are very small (see section 3.2). Based on general understanding, the fine HAZ microstructure will have mechanical properties that are equivalent to, or exceed, those of the wrought base material. Therefore, the HAZ will have mechanical properties that exceed the required minimum properties of the associated wrought material.

Two potential issues arise from welding of the absorber section: (1) sensitization and (2) residual stress. These issues are addressed below:

*Sensitization*: The low heat input laser welding processes have minimal impact on the wrought tube material, in that they typically do not result in sensitized material. To confirm this conclusion, the processes are continually evaluated metallographically to confirm the acceptability of the weld region (i.e., lack of sensitization). In addition, [[

]]. Note also from section 3.6.2 that these contact hoop stresses (and associated strains) have been eliminated for the ESBWR Marathon control rod.

*Residual stress*: One major effect of the welding process is that it will introduce tensile residual stresses in the narrow weld/HAZ region. These stresses are not a significant concern for two reasons: (1) The field cracking has not been associated with the weld HAZ and (2) the irradiation experienced by the CRB over the initial time of operation can significantly reduce these stresses by 60% or more through radiation creep processes (Reference 10). At this level of reduced stress, there is little concern for any effect on stress corrosion cracking (SCC) initiation or their applied stresses and strains. In that the major concern are strains from swelling, this level of stress is well below those levels required to even produce yielding. See also section 3.2.

Absorber Tube Expansion

The pressurization of the absorber tubes will cause an axial expansion of the tubes. This is due to the internal pressure pushing against the end plugs that seal the ends of the absorber tubes. Using the maximum allowable internal pressure, the area of the end plugs, and the number of pressurized tubes in the absorber section, the maximum axial load is calculated and shown in Table 3-19.

Assuming stresses remain in the elastic range, the axial strain on the absorber tubes is calculated as $\varepsilon = \sigma/E = P/AE$, with the elongation being $\Delta L = \varepsilon L$. For an absorber section that is nominally [[ ]] long, the total elongation is also shown in Table 3-19. These maximum elongations are relatively small, and will not affect the fit, form or function of the control rod.

Effect of Irradiated Material

The pressurization finite element model uses unirradiated material properties. To test the assertion that the use of unirradiated properties in the pressurization finite element model is conservative, two test cases are performed using irradiated material properties: (1) the single tube model used to establish the burst pressure, and (2) the model incorporating the absorber tube to tie rod weld. For each test, the unscaled burst pressure of [[ ]] (Table 3-21) is applied. Resulting peak stress and strain intensities are determined, and are compared to material allowables in Table 3-21.

As shown in Table 3-21, the resulting stress and strain intensities are less than the material ultimate values. Since the [[ ]] burst pressure is based on the unirradiated material reaching the true ultimate stress, it may be stated that the unirradiated material analysis for absorber tube pressurization is generically conservative.

### 3.6.5 Irradiation Assisted Stress Corrosion Cracking Resistance

In order for the stress corrosion cracking mechanism to activate it requires a material that is susceptible, a conducive environment and a sustained tensile stress. If one of these three mechanisms is not present to a sufficient degree, the likelihood of a stress corrosion crack to form is significantly reduced.

The Marathon absorber tube is made from a GEH proprietary stainless steel, "Rad Resist 304S", which is optimized to be resistant to Irradiation Assisted Stress Corrosion Cracking (IASCC). The chemistry of this material is shown in Section 3.2.4.

In addition to using IASCC resistant material, the ESBWR Marathon control rod is designed such that the swelling of the boron carbide capsule does not impart a mechanically imposed stress/strain on the absorber tube. See section 3.6.2. This significantly reduces the amount of stress/strain present in the absorber tubes at the end of life, and significantly reduces the likelihood of stress-corrosion cracking.

## 3.7 HANDLING LOADS

The ESBWR Marathon control rod is designed to accommodate three times the weight of the control rod during handling, to account for dynamic loads. The handle is analyzed using a finite element model, using worst-case geometry (see Figure 3-6). Table 3-11 shows the results of the handle loads analysis.

## 3.8 FATIGUE

The ESBWR control rod is designed to withstand load combinations including anticipated operational occurrences (AOOs) and fatigue loads associated with those combinations. The fatigue analysis is based on the following assumed lifetime:

[[

]]

For scram, each cycle represents a single scram insertion. Scram simulations show that the oscillations in the control rod structure damp out quickly. Further, it is extremely conservative to assume [[ ]] scrams with a 100% inoperative control rod drive buffer, as the loads experienced by the control rod in a normal buffered scram are much less severe.

For the Safe Shutdown Earthquake (SSE), a total of [[ ]] seismic events is assumed, in which each event consists of [[ ]] cycles of control rod lateral bending. The assumption of [[ ]] lifetime SSE events is also considered very conservative.

Based on the reactor cycles, the combined loads are then evaluated for the cumulative effect of maximum cyclic loadings. The fatigue usage is evaluated against a limit of 1.0. The maximum cyclic stress is determined using a conservative stress concentration factor of 3.0 for welded connections. Table 3-12 shows the fatigue usage due to control rod SCRAM at six locations. In this analysis, it is assumed that each scram occurs with a 100% failed FMCRD buffer.

Table 3-13 shows the fatigue usage at the control rod outer edge due to bending from SSE seismic events and severe channel bow, control rod scram, and maximum absorber tube internal pressure. As can be seen, the combined fatigue usage is much less than 1.0.

Table 3-14 shows the fatigue usage at the tie rod to first absorber tube weld. The combined loading due to failed buffer scram, maximum absorber tube internal pressure, SSE seismic events and severe channel bow is considered. As shown, the combined fatigue usage is much less than 1.0.

It is well known that the cycles for fatigue initiation are dependent on the stress or strain range. The stress amplitudes are all in the elastic range. As shown in Tables 3-12 through 3-14, based upon the ASME Section III fatigue design curve for un-irradiated austenitic material (Reference 6), the low number of cycles represents only a small amount of cumulative damage, well below the design limit. The ½ ultimate tensile stress value represents the ASME design limit for ~30,000 cycles. It has been established that an increase in the strength level, consistent with the effect of irradiation, would only increase the margin. This is supported by data on high strength materials, which confirm that the endurance limit is close to ½ ultimate tensile stress (Reference 7).

The last consideration with regard to fatigue is an evaluation of whether there is any flow-induced vibration that could in turn provide the potential for fatigue initiation. An assessment was performed to evaluate the loads induced by transverse loading. The evaluation that treated the control blade as a cantilever beam, found that the loads were very small and would not be sufficient to even close the gap between the blade and the fuel assembly. This load is considered so small as to be negligible, and would not lead to any risk of fatigue.

## 3.9 CONTROL ROD MECHANICAL LIFETIME

As discussed in Section 3.6, the lifetime limiting mechanism for the ESBWR Marathon control rod is [[ ]]. An absorber tube mechanical limit as a function of average B-10 per cent depletion is calculated based on peak heat generation, temperatures and helium release fractions, combined with worst-case component geometries. As discussed in Section 3.6, the method for evaluating the swelling phenomenon of irradiated boron carbide is very conservative, using worst-case capsule and absorber tube dimensions, along with a +3σ upper limit swelling rate assumption. Using these conservatisms, the ESBWR Marathon capsule is designed to result in a clearance between the absorber tube and capsule and 100% local depletion, thereby eliminated swelling induced strain in the outer absorber tube.

The calculation of the control rod mechanical lifetime limit, in terms of a four-segment average B-10 depletion, is shown in Table 3-23. Along the top of the table is the absorber tube number, where tube 1 is the first absorber tube, welded to the cruciform tie rod. Also shown are the span-wise radial peaking factors, which show the relative absorption rate of each absorber tube. A limiting axial depletion profile is used to calculate the B-10 depletion for each absorber tube and axial node. At the bottom of the table, the average depletion for each tube is shown, along with the depletion limit for that tube, which varies depending on the number of empty capsule plenums employed at the bottom of the absorber column. Through an iterative process, the peak ¼ segment depletion is raised until the limiting absorber tube reaches its mechanical limit. The 4-segment mechanical lifetime of the control rod is then the average of the four ¼ segments.

As shown in Table 3-23, the 4-segment mechanical lifetime limit is [[ ]]. From Reference 5, the ¼-segment nuclear depletion limit is [[ ]]. [[ ]], the nuclear lifetime of the ESBWR Marathon control rod is limiting, in that the mechanical lifetime exceeds the nuclear lifetime.

**Table 3-1**
**ESBWR Marathon Material Properties**

| Material Type | Control Rod Components | Ultimate Tensile Strength, $S_U$ (ksi) | | Yield Strength, $S_Y$ (ksi) | | Modulus of Elasticity, E (x $10^6$ psi) | | Poisson's Ratio, v | |
|---|---|---|---|---|---|---|---|---|---|
| | | 70 °F | 550 °F | 70 °F | 550 °F | 70 °F | 550 °F | 70 °F | 550 °F |
| 316 Plate | Handles and pads | [[ | | | | | | | |
| 316 Bar | Handle pads | | | | | | | | |
| XM-19 Bar | Connector socket | | | | | | | | |
| CF3 Casting | Connector casting | | | | | | | | |
| ER 308L | Capsule end caps, absorber tube end plugs, weld filler metal | | | | | | | | |
| 304S Bar | Tie rods | | | | | | | | |
| 304S Tubing | Absorber Tubes | | | | | | | | |
| Hardened 304L Tubing | Capsule body tubes | | | | | | | | ]] |

## Table 3-2
## Design Allowable Stresses for Primary Loads

| Material Type | CR Components | ½ Ultimate Tensile Stress $S_m$ (ksi) | |
|---|---|---|---|
| | | 70 °F | 550 °F |
| 316 Plate | Handles and pads | [[ | |
| 316 Bar | Handle pads | | |
| XM-19 Bar | Connector socket | | |
| CF3 Casting | Connector casting | | |
| ER 308L | Capsule end caps, absorber tube end plugs, weld filler metal | | |
| 304S Bar | Tie rods | | |
| 304S Tubing | Absorber Tubes | | |
| Hardened 304L Tubing | Capsule body tubes | | ]] |

**Table 3-3**
**Weld Quality Factors**

| Weld | Weld Inspection | Weld Quality Factor, q |
|---|---|---|
| Socket to Connector | [[ | |
| Connector to Absorber Section | | |
| Handle to Absorber Section | | |
| End Plug to Absorber Tube | | ]] |

**Table 3-4**
**Maximum Control Rod Failed Buffer SCRAM Dynamic Loads**

| Components | Maximum Equivalent Loads in Kips ($10^3$ lbs) | |
|---|---|---|
| | 70 °F | 550 °F |
| Coupling | [[ | |
| Connector | | |
| Connector/Absorber Section Interface | | |
| Absorber Section | | |
| Handle/Absorber Section Interface | | ]] |

**Table 3-5**
**ESBWR Marathon Failed Buffer SCRAM Stresses**

| Location (Figure 3-1 Section) | Room Temperature (70 °F) | | | Operating Temperature (550 °F) | | |
|---|---|---|---|---|---|---|
| | Maximum Stress | Allowable Limit | Design Ratio | Maximum Stress | Allowable Limit | Design Ratio |
| Socket Minimum Cross-Sectional Area (A-A) | [[ | | | | | |
| Socket to Connector Weld (B-B) | | | | | | |
| Connector Minimum Cross-Sectional Area (C-C) | | | | | | |
| Connector to Absorber Section Weld (D-D) | | | | | | |
| Absorber Section (E-E) | | | | | | |
| Handle to Absorber Section Weld (F-F) | | | | | | ]] |

**Table 3-6**
**Outer Edge Bending Strain due to Seismic and Channel Bow Bending, Internal Absorber Tube Pressure and Failed Buffer Scram**

| Description | Value at 550 °F |
|---|---|
| Outer Edge Bending Strain, Seismic (%) | [[ |
| Outer Edge Bending Strain, Seismic + Channel Bow (%) | |
| Max Internal Pressure Axial Stress (ksi) | |
| Max Failed Buffer Scram Stress (ksi) | |
| Total Outer Edge Strain, Seismic + Failed Buffer Scram + Absorber Tube Internal Pressure (%) | |
| Total Outer Edge Strain, Seismic + Channel Bow + Failed Buffer Scram + Absorber Tube Internal Pressure (%) | |
| Allowable Strain (%) ½ Ultimate, Irradiated | |
| Design Ratio | ]] |

**Table 3-7**
**Absorber Tube to Tie Rod Weld Stress**

| Description | Value at 550 °F |
|---|---|
| Seismic + Internal Pressure, Max $S_{INT}$ (ksi) | [[ |
| Seismic + Channel Bow + Internal Pressure, Max $S_{INT}$ (ksi) | |
| True Ultimate Tensile Stress (ksi) | |
| Design Ratio | ]] |

**Table 3-8**
**Stuck Rod Compression Buckling – Entire Control Rod (Mode A)**

| Description | 70 °F | 550 °F |
|---|---|---|
| Critical Buckling Load, $P_{cr}$ (lb) | [[ | |
| Compressive Yield Load (lb) | | |
| Maximum Stuck Rod Compression Load (lb) | | |
| Design Ratio,Buckling | | |
| Design Ratio, Compressive Yield | | ]] |

**Table 3-9**
**Stuck Rod Compression Buckling – Control Rod Wing (Mode B)**

| Description | 70 °F | 550 °F |
|---|---|---|
| Critical Buckling Load, $P_{cr}$ (lb) | [[ | |
| Compressive Yield Load (lb) | | |
| Total Compressive Load (lb) | | |
| Design Ratio, Buckling | | |
| Design Ratio, Compressive Yield | | ]] |

**Table 3-10**
**Boron Carbide Peak Temperatures and Helium Release Fractions**

| **Parameter** | **Nominal Dimensions** | **Worst Case Dimensions** |
|---|---|---|
| $B_4C$ Centerline Temperature (°F) | [[ | |
| Average $B_4C$ Temperature (°F) | | |
| Helium Release Fraction (%) | | ]] |

**Table 3-11**
**Handle Lifting Load Stress**

| **Description** | **Value at 70 °F** |
|---|---|
| Maximum Equivalent Stress (ksi) | [[ |
| Allowable Stress (ksi) | |
| Design Ratio | ]] |

**Table 3-12**
**Fatigue Usage due to Failed Buffer Scram**

| Location | Stress Amp. (ksi) | Allowable Cycles (N) | Actual Cycles | Usage |
|---|---|---|---|---|
| Socket Minimum Area | [[ | | | |
| Socket to Connector Weld | | | | |
| Connector to Absorber Section Weld | | | | |
| Absorber Section | | | | |
| Handle to Absorber Section Weld | | | | ]] |

**Table 3-13**
**Fatigue Usage at Absorber Section Outer Edge**

| Stress Type | Stress Amp. (ksi) | Allowable Cycles (N) | Actual Cycles | Usage |
|---|---|---|---|---|
| Absorber Section Outer Edge - Scram + Internal Pressure | [[ | | | |
| Absorber Section Outer Edge – Seismic + Channel Bow | | | | ]] |
| | Total Usage = | | [[ | ]] |

**Table 3-14**
**Fatigue Usage at Absorber Tube to Tie Rod Weld**

| Stress Type | Stress Amp. (ksi) | Allowable Cycles (N) | Actual Cycles | Usage |
|---|---|---|---|---|
| Absorber Tube to Tie Rod Weld - Scram | [[ | | | |
| Absorber Tube to Tie Rod Weld – Seismic + Channel Bow + Internal Pressure | | | | ]] |
| | Total Usage = | | [[ | ]] |

**Table 3-15**
**Irradiated Boron Carbide Diametral Swelling Data**

[[

| | |
|---|---|
| | |
| | |
| | |
| | |
| | |
| | |
| | |
| | |
| | |
| | |
| | |
| | |
| | |
| | |
| | |
| | |
| | |
| | |
| | |
| | |
| | |
| | |
| | |
| | |

]]

**Table 3-16**
**Irradiated Boron Carbide Axial Swelling Data**

[[

| | |
|---|---|
| | |
| | |
| | |

]]

**Table 3-17**
**Irradiated Boron Carbide Capsule Swelling Calculation**

| Parameter | Value |
|---|---|
| Absorber Tube ID Before Welding (in) | [[ |
| **Minimum Absorber Tube ID After Welding (in)** | |
| Capsule OD (in) | |
| Capsule Wall Thickness (in) | |
| Maximum Capsule $OD_0$ (in) | |
| Maximum Capsule $ID_0$ (in) | |
| Capsule ID strain (in/in) | |
| Capsule OD strain (in/in) | |
| **Capsule OD at 100% local depletion** | ]] |

**Table 3-18**
**Absorber Tube Pressurization Results: Principle Stress Results at Operating Temperature and Pressure and Maximum Allowable Pressure**

| Stress Component | Value |
|---|---|
| S1 (Hoop) | [[ |
| S2 (Axial) | |
| S3 (Radial) | |
| Equivalent Stress | |
| Allowable Stress | ]] |

**Table 3-19**
**Control Rod Axial Elongation due to Absorber Tube Pressurization**

| Parameter | Value |
|---|---|
| Axial Load due to Pressurization (kips) | [[ |
| Absorber Section Cross-Sectional Area ($in^2$) | |
| Modulus of Elasticity, E (ksi) | |
| Strain (in/in) | |
| Elongation, ΔL (inch) | ]] |

**Table 3-20**
**Absorber Tube Burst and Allowable Pressures at 550 °F**

| Parameter | Pressure (psia) |
|---|---|
| FEA Burst Pressure, Nominal Dimensions | [[ |
| FEA Burst Pressure, Tie Rod Model | |
| FEA Burst Pressure, Worst-Case Dimensions | |
| **Scaled Burst Pressure (7% reduction to match burst pressure tests)** | |
| **Allowable Pressure (2.0 Safety Factor)** | ]] |

**Table 3-21**
**Absorber Tube Pressurization Using Irradiated Material**

| Case | Peak Stress Intensity (ksi) | True Ultimate Stress (ksi) | Peak Total Strain Intensity (%) | True Ultimate Tensile Strain (%) |
|---|---|---|---|---|
| Single Tube, Irradiated | [[ | | | |
| Tube and Tie Rod, Irradiated | | | | ]] |

**Table 3-22**
**Type 304S Absorber Tube Mechanical Properties**

| Property | Room Temperature Yield Stress (ksi) | 550 °F Yield Stress (ksi) | Room Temperature Ultimate Tensile Stress (ksi) | 550 °F Ultimate Tensile Stress (ksi) | Room Temperature Elongation (% in 2 inches) |
|---|---|---|---|---|---|
| Specification Requirement* | [[ | | | | |
| Example Lot 1 | | | | | |
| Example Lot 2 | | | | | |
| Example Lot 3 | | | | | ]] |

* These material requirements are specified in the fabrication specification for the absorber tubes. The tubing supplier certifies each lot of absorber tubes as meeting these requirements.

**Table 3-23**
**Mechanical Lifetime Calculation**

[[

]]

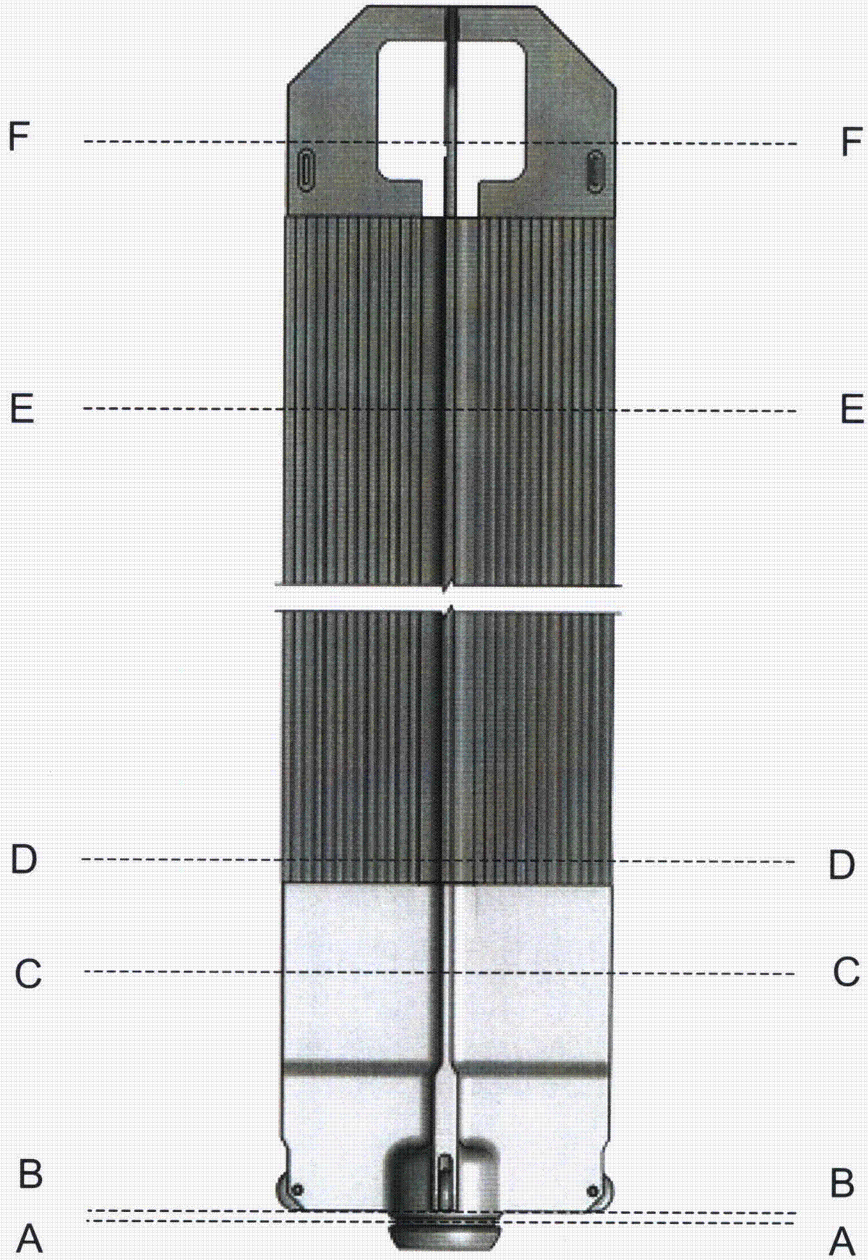


**Figure 3-1. Control Rod Assembly Welds and Cross-Sections Analyzed for SCRAM**

[[

]]

**Figure 3-2. Absorber Tube to Tie Rod Finite Element Model**

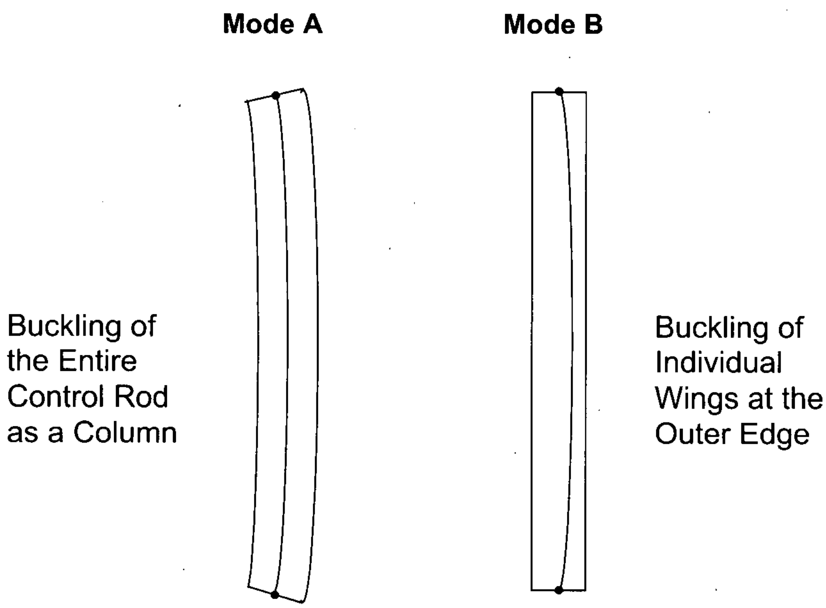


**Figure 3-3. Control Rod Buckling Modes**

[[

]]

**Figure 3-4. Absorber Tube Pressurization Finite Element Model**

[[

]]

**Figure 3-5. Absorber Tube and Capsule Thermal Finite Element Model**

[[

]]

**Figure 3-6. Handle Lifting Loads Finite Element Model**

[[

]]

**Figure 3-7. Irradiated Test Capsule Configurations**

[[

]]

**Figure 3-8. Irradiated Boron Carbide Diametral Swelling Data**

[[

]]

**Figure 3-9. Neutron Radiograph of Irradiated Marathon Absorber Capsules**

[[

]]

**Figure 3-10. Tube Pressurization Finite Element Model, Tube + Tie Rod**

[[

]]

**Figure 3-11. Lateral Load Finite Element Model**

[[

]]

**Figure 3-12. Lateral Load Finite Element Results**

[[

]]

**Figure 3-13. Absorber Tube Material, 300X Magnification**

[[

]]

**Figure 3-14. Absorber Tube Material, 300X Magnification**

[[

]]

**Figure 3-15. Absorber Tube Material, 300X Magnification**

[[

]]

**Figure 3-16. Typical Autogenous Laser Weld of 304S Absorber Tube**

# 4. LICENSING CRITERIA

The Design Control Document for ESBWR (Reference 4) identifies four criteria for the licensing and evaluation of the ESBWR control rod. These criteria are evaluated as follows.

## 4.1 STRESS, STRAIN, AND FATIGUE

### 4.1.1 Criteria

Control rod stresses, strains, and cumulative fatigue are evaluated to not exceed the ultimate stress or strain limit of the material, structure, or welded connection.

### 4.1.2 Conformance

As discussed in Section 3, the ESBWR Marathon design has been evaluated using the same or more conservative design bases and methodology than the Marathon CRB. All components of the control rod are found to be acceptable when analyzed for stresses due to normal, abnormal, emergency, and faulted loads. The design ratio, which is the effective stress divided by the stress limit or the effective strain divided by the strain limit, is found to be less than or equal to 1.0 for all components. Conservatism is included in the evaluation by limiting stresses for all primary loads to one-half of the ultimate strength (i.e., a safety factor of two is employed).

The fatigue usage of the ESBWR Marathon control rod is calculated using the same methodology as the Marathon CRB. The fatigue analysis assumes [[ ]]. It is found that the calculated fatigue usage is less than the material fatigue capability (the fatigue usage factor is much less than 1.0).

## 4.2 CONTROL ROD INSERTION

### 4.2.1 Criteria

The control rod design is evaluated to be capable of insertion into the core during all modes of plant operation within the limits assumed in the plant analyses.

### 4.2.2 Conformance

The ESBWR Marathon control rod is designed to withstand maximum stresses and strains experienced during control rod insertion, including scram. Section 3 demonstrates the structural acceptability of the ESBWR Marathon control rod.

The ability of the ESBWR Marathon control rod to insert into the core within acceptable scram times is discussed in section 4.2.4.2 of the ESBWR Tier 2 DCD (Reference 4). The worst-case scenario for a control rod scram within scram time requirements is a scram during a seismic event. As discussed in the ESBWR Tier 2 DCD (Reference 4), an ABWR Marathon control rod was tested during scram with simulated seismic fuel channel oscillation. This ABWR Marathon control rod inserted within scram time requirements, and suffered no detrimental damage. As noted in the ESBWR Tier 2 DCD (Reference 4), the ESBWR Marathon control rod seismic conditions are bounded by the ABWR test.

## 4.3 CONTROL ROD MATERIAL

### 4.3.1 Criteria

Control rod materials are shown to be compatible with the reactor environment.

### 4.3.2 Conformance

No new materials are introduced for the ESBWR Marathon control rod that have not been used in control rods in operating BWR/2-6 plants. The ESBWR Marathon control rod is designed to be crevice-free, and uses materials resistant to corrosion and stress corrosion cracking. For example, the absorber tubes are made from the same high purity, stabilized type 304S stainless steel as BWR/2-6 Marathon control rods. This material was developed by GEH to be resistant to stress corrosion cracking.

## 4.4 REACTIVITY

### 4.4.1 Criteria

Control rod reactivity worth shall be included in the plant core analyses.

### 4.4.2 Conformance

As discussed in Section 1 of Reference 5, the equilibrium core design for ESBWR was performed using a BWR/6 (S lattice) original equipment control rod. As also discussed in Reference 5, the compatibility of the ESBWR Marathon control rod is ensured by matching the initial cold reactivity worth of the Marathon CRB with the BWR/6 original equipment used in the core design.

# 5. SURVEILLANCE

As directed by NRC, the following is the proposed surveillance program for the ESBWR Marathon control rod.

With the assistance of the BWR plant sites, GEH will monitor the depletions of installed ESBWR Marathon control rods and will make arrangements to visually inspect the four highest depletion control rods during each refueling outage until the control rods have reached as close to end of life as practical and are removed from the high depletion locations.

Should evidence of a problem with material integrity arise; (1) arrangements will be made to inspect additional control rods to the extent necessary to identify the root cause and (2) if appropriate, GEH will recommend a revised lifetime limit to the NRC based on the inspections and other applicable information.

GEH will report to NRC the status of the ESBWR Marathon control rod surveillance program, including the results of all visual inspections, at least annually following the end of the first cycle of ESBWR operation.

# 6. REFERENCES

1. GE Nuclear Energy, "GE Marathon Control Rod Assembly," NEDE-31758P-A, GE Proprietary, October 1991.

2. GE Nuclear Energy, "Safety Evaluation of the General Electric Duralife 230 Control Rod Assembly," NEDE-22290-P-A Supplement 3, GE Proprietary, May 1988.

3. GE Nuclear Energy, "Marathon-5S Control Rod Assembly", NEDE-33284P, GE Proprietary, September 2006.

4. GE-Hitachi Nuclear Energy, "ESBWR Design Control Document Tier 2, Chapter 4, Reactor", 26A6642AP, GEH Proprietary.

5. GE-Hitachi Nuclear Energy, "Licensing Topical Report: ESBWR Control Rod Nuclear Design", NEDE-33243 Rev. 1, GEH Proprietary, October 2007.

6. 1989 ASME Section III, Division 1, Appendix I, Figure I-9.2.1.

7. JA Bannantine, JJ Comer and JL Handrock, 'Fundamentals of Metal Fatigue Analysis', Prentice Hall, 1990.

8. BWR Vessel and Internals Project: Fracture Toughness and Tensile Properties of Irradiated Austenitic Stainless Steel Components Removed from Service (BWRVIP-35)," EPRI TR-108279, June 1997.

9. BWR Vessel and Internals Project: Review of Test Data for Irradiated Stainless Steel Components (BWRVBIP-66)," EPRI TR-112611, March 1999.

10. "Boiling Water Reactor Vessel and Internal Project: Crack Growth Rates in Irradiated Stainless Steels in BWR Internal Components (BWRVIP-99)", EPRI TR 1003018 Final Report, December 2001.

11. *Mechanical Behavior of Materials*, F. A. McClintock and A. S. Argon, pages 277-278, Addison-Wesley Publishing Company, Inc., 1966.

# A. APPENDIX A – FAILED BUFFER SCRAM STRESS EVALUATION

Failed buffer scram stress calculations for all cross-sections shown in Figures 3-1 and 3-2 are shown in Table 3-5. During a control rod scram, large axial loads are imparted on the control rod. These axial loads are determined using a dynamic spring and mass model, the results of which are presented in Table 3-4. For this analysis, the scram loads are determined assuming a 100% inoperative control rod drive buffer. The following cross-sections are analyzed.

## A-1 SOCKET MINIMUM CROSS-SECTIONAL AREA (FIG. 3-1, SECTION A-A)

The minimum cross-sectional area of the socket is calculated from the drawing to be [[ ]]. Actual and allowable stress calculations are shown in Table A-1. As shown, all design ratios are less than 1.0. Therefore, the structure is acceptable.

## A-2 SOCKET TO CONNECTOR WELD (FIG. 3-1, SECTION B-B)

The socket is screwed into the connector casting, and sealed using a circumferential fillet weld. The weld joins the XM-19 socket to the type CF3 connector casting, with ER 308L filler metal required. The minimum, combined effective normal area for this connection is calculated to be [[ ]]. Table A-2 calculates the actual and allowable stresses for this weld. As shown, all design ratios are less than 1.0. Therefore, the weld is acceptable.

## A-3 CONNECTOR MINIMUM CROSS-SECTIONAL AREA (FIG. 3-1, SECTION C-C)

The minimum cross-sectional area of the connector is calculated from the drawing to be [[ ]]. Actual and allowable stress calculations are shown in Table A-3. As shown, all design ratios are less than 1.0. Therefore, the structure is acceptable.

## A-4 CONNECTOR TO ABSORBER SECTION WELD (FIG. 3-1, SECTION D-D)

The weld connecting the absorber section to the connector is analyzed using the combined loading of the scram loads and axial loads due to the maximum allowable internal pressure of the absorber tubes.

Since both the scram loads and the load due to the internal pressure of the absorber tubes is considered, a combined weld area of the absorber section to connector weld, and the end plug to absorber tube weld is calculated. Since the end plug weld is in shear for this loading, the weld area is multiplied by $(1/\sqrt{3})$ to calculate an effective normal weld area. This is added to the minimum absorber section to connector weld area, which is determined using CAD software:

$A_{normal}$ = (# of tubes}{$(1/\sqrt{3})(\pi)OD_{plug,min}$(weld penetration) + (absorber section to handle/connector area per tube)}.

The weld area per tube is then multiplied by the number of tubes. The weld area calculation is summarized in Table A-4.

Once the effective normal weld area is known, the combined maximum stresses due to scram and internal pressure are calculated as described in Table A-5. As shown, all design ratios are less than 1.0. Therefore, the weld is acceptable.

## A-5 ABSORBER SECTION (FIG. 3-1, SECTION E-E)

The minimum cross-sectional area of the absorber section is calculated in Table A-6. Actual and allowable stresses are shown in Table A-7. As shown, all design ratios are less than 1.0. Therefore, the structure is acceptable.

## A-6 ABSORBER SECTION TO HANDLE WELD (FIG. 3-1, SECTION F-F)

The weld connecting the absorber section to the handle is analyzed using the combined loading of the scram loads and axial loads due to the maximum allowable internal pressure of the absorber tubes.

The effective weld area calculation is identical to the calculation in Table A-4 for the connector to absorber section weld. Using this effective normal weld area, the combined maximum stresses due to scram and internal pressure are calculated as described in Table A-8. As shown, all design ratios are less than 1.0. Therefore, the structure is acceptable.

**Table A-1. Socket Axial Stress Calculations**

| Description | Source | 70 °F | 550 °F |
|---|---|---|---|
| Max Failed Buffer Scram Load (kips) | Table 3-4 | [[ | |
| Max Failed Buffer Scram Stress (ksi) | [[ ]] | | |
| Allowable Stress (ksi) | Table 3-2 (XM-19) | | |
| **Design Ratio** | =stress/allow | | ]] |

**Table A-2. Socket to Connector Weld Stress Calculations**

| Description | Source | 70 °F | 550 °F |
|---|---|---|---|
| Max Failed Buffer Scram Load (kips) | Table 3-4 | [[ | |
| Max Failed Buffer Scram Stress (ksi) | [[ ]] | | |
| Allowable Stress (ksi) | Table 3-2 (CF3) | | |
| **Design Ratio** | =stress/allow | | ]] |

**Table A-3. Minimum Connector Area Stress Calculations**

| Description | Source | 70 °F | 550 °F |
|---|---|---|---|
| Max Failed Buffer Scram Load (kips) | Table 3-4 | [[ | |
| Max Failed Buffer Scram Stress (ksi) | [[ ]] | | |
| Allowable Stress (ksi) | Table 3-2 (CF3) | | |
| **Design Ratio** | =stress/allow | | ]] |

**Table A-4. Connector to Absorber Section Weld Geometry**

| Description | Reference | Value |
|---|---|---|
| Absorber Tube to Connector Weld Area ($in^2$) | CAD analysis | [[ |
| Min End Plug OD (in) | Drawing | |
| Max End Plug OD (in) | Drawing | |
| Min End Plug Weld Penetration (in) | Assembly Drawing | |
| Total Normal Weld Area Per Tube | CAD Analysis | |
| Number of Absorber Tubes per Assembly | Assembly Drawing | |
| Total Weld Area ($in^2$) | =(# tubes)(area) | ]] |

**Table A-5. Connector to Absorber Section Weld Stress Calculations**

| Description | Source | 70 °F | 550 °F |
|---|---|---|---|
| Max Failed Buffer Scram Load (kips) | Table 3-4 | [[ | |
| Maximum Allowable Internal Pressure (ksi) | Finite Element Analysis | | |
| End Plug Pressure Area (in$^2$) | $=\pi/4*(OD_{plug})^2$ | | |
| Number of Pressurized Tubes | Assembly Drawing | | |
| Total Axial Load (kips) | =Scram Load + (press)(area) (# tubes) | | |
| Total Weld Area (in$^2$) | Table A-4 | | |
| Max Failed Buffer Scram + Internal Pressure Stress (ksi) | =Ptot/A | | |
| Allowable Stress (ksi) | Table 3-2 (CF3/304S Tubes) | | |
| Weld Quality Factor | Table 3-3 | | |
| Allowable Weld Stress (ksi) | $=S_m*q$ | | |
| **Design Ratio** | =Stress/Allow | | ]] |

**Table A-6. Absorber Section Geometry Calculation**

| Description | Source | Value |
|---|---|---|
| Min Absorber Tube Area (in$^2$) | CAD Analysis | [[ |
| Min Tie Rod Area (in$^2$) | CAD Analysis | |
| Number of Absorber Tubes | Assembly Drawing | |
| Total Minimum Absorber Section Cross-sectional Area (in$^2$) | =(# tubes)(tube area) + tie rod area | ]] |

**Table A-7. Absorber Section Stress Calculation**

| Description | Source | 70 °F | 550 °F |
|---|---|---|---|
| Max Failed Buffer Scram Load (kips) | Table 3-4 | [[ | |
| Max Failed Buffer Scram Stress (ksi) | =P/A | | |
| Allowable Stress (ksi) | Table 3-2 (304S Tubes) | | |
| **Design Ratio** | =stress/allow | | ]] |

**Table A-8. Absorber Section to Handle Weld Stress Calculations**

| Description | Source | 70 °F | 550 °F |
|---|---|---|---|
| Max Failed Buffer Scram Load (kips) | Table 3-4 | [[ | |
| Maximum Allowable Internal Pressure (ksi) | Finite Element Analysis | | |
| End Plug Pressure Area (in$^2$) | $=\pi/4*(OD_{plug})^2$ | | |
| Number of Pressurized Tubes | From assembly drawing | | |
| Total Axial Load (kips) | =Scram Load + (press)(area)(# tubes) | | |
| Total Weld Area (in$^2$) | Table B-10 | | |
| Max Failed Buffer Scram + Internal Pressure Stress (ksi) | =Ptot/A | | |
| Allowable Stress (ksi) | Table 3-2 (304S Tubes) | | |
| Weld Quality Factor | Table 3-3 | | |
| Allowable Weld Stress (ksi) | $=S_m*q$ | | |
| **Design Ratio** | =Stress/Allow | | ]] |

**MFN 07-612**

**Enclosure 3**

**Affidavit**

# GE Hitachi Nuclear Energy

## AFFIDAVIT

**I, David H. Hinds,** state as follows:

(1) I am General Manager, New Units Engineering, GE Hitachi Nuclear Energy ("GEH") and have been delegated the function of reviewing the information described in paragraph (2) which is sought to be withheld, and have been authorized to apply for its withholding.

(2) The information sought to be withheld is contained in the GEH proprietary report NEDE-33244P, *ESBWR Marathon Control Rod Mehanical Design Report,* Revision 1, Class III (GEH Proprietary Information), dated November 2007. GEH proprietary information is identified by a dark red font with dotted underline inside double square brackets. Figures and large equation objects are identified with double square brackets before and after the object. In each case, the superscript notation {3} refers to Paragraph (3) of this affidavit, which provides the basis for the proprietary determination.

(3) In making this application for withholding of proprietary information of which it is the owner, GEH relies upon the exemption from disclosure set forth in the Freedom of Information Act ("FOIA"), 5 USC Sec. 552(b)(4), and the Trade Secrets Act, 18 USC Sec. 1905, and NRC regulations 10 CFR 9.17(a)(4), and 2.390(a)(4) for "trade secrets" (Exemption 4). The material for which exemption from disclosure is here sought also qualify under the narrower definition of "trade secret", within the meanings assigned to those terms for purposes of FOIA Exemption 4 in, respectively, Critical Mass Energy Project v. Nuclear Regulatory Commission, 975F2d871 (DC Cir. 1992), and Public Citizen Health Research Group v. FDA, 704F2d1280 (DC Cir. 1983).

(4) Some examples of categories of information, which fit into the definition of proprietary information, are:

a. Information that discloses a process, method, or apparatus, including supporting data and analyses, where prevention of its use by GEH's competitors without license from GEH constitutes a competitive economic advantage over other companies;

b. Information which, if used by a competitor, would reduce his expenditure of resources or improve his competitive position in the design, manufacture, shipment, installation, assurance of quality, or licensing of a similar product;

c. Information, which reveals aspects of past, present, or future GEH customer-funded development, plans and programs, resulting in potential products to GEH;

d. Information, which discloses patentable subject matter for which it may be desirable to obtain patent protection.

The information sought to be withheld is considered to be proprietary for the reasons set forth in paragraphs (4)a., and (4)b, above.

(5) To address 10 CFR 2.390 (b) (4), the information sought to be withheld is being submitted to NRC in confidence. The information is of a sort customarily held in confidence by GEH, and is in fact so held. The information sought to be withheld has, to the best of my knowledge and belief, consistently been held in confidence by GEH, no public disclosure has been made, and it is not available in public sources. All disclosures to third parties including any required transmittals to NRC, have been made, or must be made, pursuant to regulatory provisions or proprietary agreements, which provide for maintenance of the information in confidence. Its initial designation as proprietary information, and the subsequent steps taken to prevent its unauthorized disclosure, are as set forth in paragraphs (6) and (7) following.

(6) Initial approval of proprietary treatment of a document is made by the manager of the originating component, the person most likely to be acquainted with the value and sensitivity of the information in relation to industry knowledge. Access to such documents within GEH is limited on a "need to know" basis.

(7) The procedure for approval of external release of such a document typically requires review by the staff manager, project manager, principal scientist or other equivalent authority, by the manager of the cognizant marketing function (or his delegate), and by the Legal Operation, for technical content, competitive effect, and determination of the accuracy of the proprietary designation. Disclosures outside GEH are limited to regulatory bodies, customers, and potential customers, and their agents, suppliers, and licensees, and others with a legitimate need for the information, and then only in accordance with appropriate regulatory provisions or proprietary agreements.

(8) The information identified in paragraph (2), above, is classified as proprietary because it contains detailed design, methodology, and dimensional information regarding the ESBWR Marathon Control Rod developed by GEH over a period of several years at a substantial cost.

The development of the testing and evaluation process along with the interpretation and application of the analytical results is derived from the extensive experience database that constitutes a major GEH asset.

(9) Public disclosure of the information sought to be withheld is likely to cause substantial harm to GEH's competitive position and foreclose or reduce the availability of profit-making opportunities. The information is part of GEH's comprehensive BWR safety and technology base, and its commercial value extends

beyond the original development cost. The value of the technology base goes beyond the extensive physical database and analytical methodology and includes development of the expertise to determine and apply the appropriate evaluation process. In addition, the technology base includes the value derived from providing analyses done with NRC-approved methods.

The research, development, engineering, analytical and NRC review costs comprise a substantial investment of time and money by GEH.

The precise value of the expertise to devise an evaluation process and apply the correct analytical methodology is difficult to quantify, but it clearly is substantial.

GEH's competitive advantage will be lost if its competitors are able to use the results of the GEH experience to normalize or verify their own process or if they are able to claim an equivalent understanding by demonstrating that they can arrive at the same or similar conclusions.

The value of this information to GEH would be lost if the information were disclosed to the public. Making such information available to competitors without their having been required to undertake a similar expenditure of resources would unfairly provide competitors with a windfall, and deprive GEH of the opportunity to exercise its competitive advantage to seek an adequate return on its large investment in developing these very valuable analytical tools.

I declare under penalty of perjury that the foregoing affidavit and the matters stated therein are true and correct to the best of my knowledge, information, and belief.

Executed on this 15th day of November 2007.

David H. Hinds
GE Hitachi Nuclear Energy